Preamble Design for Joint Frame Synchronization, Frequency Offset Estimation and Channel Estimation in Burst Mode Coherent PONs

Yongxin Sun*, Hexun Jiang*, Lilin Yi, Weisheng Hu, and Qunbi Zhuge※

State Key Laboratory of Advanced Optical Communication Systems and Networks, Department of Electronic Engineering, Shanghai Jiao Tong University, Shanghai, 200240, China

**Equal contributions*

※Corresponding author: qunbi.zhuge@sjtu.edu.cn

Abstract: We propose a preamble jointly achieving frame synchronization, frequency offset and channel estimation for burst-mode detection in coherent PON. The DSP converges within a 272-symbol preamble in a 15 GBaud experiment.

1. Introduction

Passive optical network (PON) is a cost-effective solution to deliver high data rate fiber access services. Currently, 50G PON based on intensity modulation and direct-detection (IMDD) is moving from standards to commercial use. When evolving towards 100G and beyond, it is challenging for IMDD systems to meet the requirement of power budget, and coherent systems are considered to be a promising solution for future PON [1].

In the coherent point-to-multipoint PON, signals in the upstream coming from different optical network units might have different optical powers, frequency offsets (FO), state of polarizations (SOP) and clocks. Therefore, conventional digital signal processing (DSP) used in point-to-point links is no longer suitable for burst-mode coherent-reception owing to its excessively long convergence time. To handle this problem, several specially designed preambles have been proposed to accelerate the DSP convergence [2-3]. Most of them are designed by combining several sequences with different functions, which is feasible but not efficient in terms of preamble length. Besides, general channel estimation merely considers a simple SOP matrix, so in extreme conditions with large differential group delay (DGD), the equalizer trained by a least mean square (LMS) algorithm still requires a long converging time. In addition, since the FO estimation (FOE) is typically executed before the SOP compensation, it is essential for FOE to demonstrate robustness to SOP variations, which has received limited attention in previous works.

In this paper, we design a preamble based on a constant amplitude zero auto-correlation (CAZAC) sequence. In contrast to prior works, the preamble offers three distinct advantages. Firstly, by jointly accomplishing frame synchronization (FS), FOE and channel estimation (CE), the length of the preamble can be reduced significantly. Secondly, both the FS and FOE have been designed to exhibit robust tolerance to SOP variations. Thirdly, the CE can effectively accelerate the equalizer convergence even in the presence of large DGD. Numerical and experimental results indicate that the preamble with a length of 272 symbols can effectively achieve accurate FS, FOE, and a fast convergence of the equalizer with the aid of the CE.

2. Principle

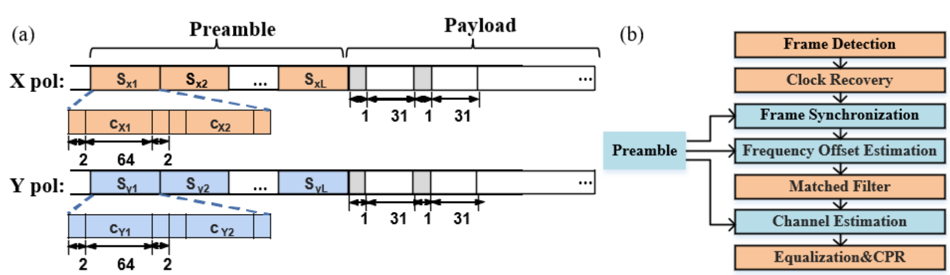

Fig. 1 (a) The proposed data frame structure. (b) Data-aided DSP flow at the receiver side for burst-mode detection.

As shown in Fig.1(a), the designed preamble contains several repeated training sequences $\boldsymbol{S}_{X/Y}$, each of which consists of four CAZAC blocks $[\boldsymbol{c}_{x1}\ \boldsymbol{c}_{x2}; \boldsymbol{c}_{y1}\ \boldsymbol{c}_{y2}]$. An ordinary CAZAC sequence can be defined by

$$c(n) = \exp(j\pi\mu n^2/N) \quad n = 1,2,\cdots N, \tag{1}$$

where N is the length of the CAZAC sequence, and μ is a prime integer to N ($\mu = 1$ in this work). The four training CAZAC blocks are rearranged as follows:

$$c_{X1} = c[1,2,\cdots N-1,N] \quad c_{X2} = c\left[N^*, N-1^*, \cdots 2^*,\ 1^*\right] \tag{2}$$

$$c_{Y1} = c[N/2+1, N/2+2, \cdots N, 1,2, \cdots N/2] \quad c_{Y2} = -c[N/2^*, N/2-1^*, \cdots 1^*, N^*, \cdots N/2+1^*] \tag{3}$$

where $*$ denotes the conjugate operation. We also add a guard interval (GI) at the beginning and the end of each block. In this preamble, every training sequence $S_{X/Y}$ can achieve FS, FOE and CE independently, and L consecutive identical training sequences $S_{X1/Y1}$, $S_{X2/Y2}, \cdots$, $S_{XL/YL}$ are designed to reduce the impact of noise. In the payload, one-symbol pilot is inserted into every 31 payload symbols for pilot-based carrier phase recovery (CPR).

Fig.1(b) depicts the DSP flow at the receiver side for burst-mode detection using the designed preamble. Frame detection is performed firstly to obtain an approximate position of the frame header. After that, the Godard algorithm is used to realize time recovery. With the aid of the preamble, FOE and FS are performed sequentially. After a matched filter, CE is utilized to initialize the equalizer tap coefficients. Equalization in the frequency domain embedded with CPR is based on the LMS algorithm, which is firstly trained by the known symbols and then switched to a decision-directed mode.

Considering that frame detection, clock recovery and CPR are independent of the properties of the proposed preamble, in the following we will mainly discuss the principles of FS, FOE and CE.

FS: The timing metric of every training sequence on each polarization is expressed by

$$C_{X/Y}(m) = \text{abs}\left[\sum_{k=0}^{N_{cazac}-1} r_{X/Y}(m+k)\, r_{X/Y}(m+2N_{cazac}-1-k)/P_{X/Y,N}\right], \tag{4}$$

where $r_{X/Y}(m)$ represents the received signal on X/Y polarization, and $P_{X/Y,N}$ represents the normalization power factor. Firstly, with the design of the conjugated and symmetrical training sequence structure, it can be proved that the FO has no impact on the peak of $C_{X/Y}$. Besides, considering the random polarization rotations after fiber transmission, we calculate another two timing metrics of $X+Y$ and $X-Y$, and then select the maximum peak to improve the robustness. If the number of training sequences is more than one, we can multiply the timing metrics of L consecutive sequences to increase the peak value of $C_{X/Y}$.

FOE: After the precise FS, a data-aided FOE is performed. For ideal SOP, received symbols can be expressed as Eq. (5), where $c(k)$ represents transmitted symbols, f_d represents FO, φ represents phase noise, T represents symbol period and $n(k)$ is Gaussian noise.

$$r_{X/Y}(k) = c_{X/Y}(k)\exp(j2\pi f_d kT + \varphi) + n(k). \tag{5}$$

It is apparent that $r_{X/Y}(k)$ depends on $c_{X/Y}(k)$, so we remove this dependence by multiplying $r_{X/Y}(k)$ by $c^*_{X/Y}(k)$ in Eq. (6). Subsequently, as discussed in [4], we calculate correlations $R_{X/Y}(m)$ shown in Eq. (7).

$$z_{X/Y}(k) = r_{X/Y}(k){c^*}_{X/Y}(k) = \exp(\mathrm{j}2\pi f_d kT + \varphi)\,[1+\tilde{n}(k)], \tag{6}$$

$$R_{X/Y}(m) = \frac{1}{L_{total}-m}\sum_{k=m+1}^{L_{total}} z_{X/Y}(k){z^*}_{X/Y}(k-m) = \exp(\mathrm{j}2\pi m f_d T)\,[1+\gamma(m)] \quad m \in [1, L_{total}/2], \tag{7}$$

where $L_{total} = L \times N_{cazac}$. Since $\tilde{n}$, γ are statistically equivalent Gaussian noise which could be neglected after averaging, we can calculate f_d from the increment of $\arg(R_{X/Y})$. When SOP is considered, new received symbols can be expressed as Eq. (8). In addition, Eq. (9) can be concluded from the definition of CAZAC in Eq. (1-3).

$$\begin{bmatrix} r'_X \\ r'_Y \end{bmatrix} = \begin{bmatrix} cos\theta e^{-j\alpha} & sin\theta e^{-j\beta} \\ -sin\theta e^{j\beta} & cos\theta e^{j\alpha} \end{bmatrix} \begin{bmatrix} r_X \\ r_Y \end{bmatrix} \tag{8}$$

$$c_Y(k) = \begin{cases} -c_X(k) & k\ is\ odd \\ c_X(k) & k\ is\ even \end{cases} \tag{9}$$

Substituting Eq. (8) and (9) into Eq. (6), we can get the final expression of $R'_{X/Y}(m)$ in (10), whose phase is largely independent of SOP. Thus, we obtain the estimated FO $\overline{f_d}$ in Eq. (11).

$$R'_{X/Y}(m) = \begin{cases} (\cos^2\theta - \sin^2\theta)\exp(\mathrm{j}2\pi m f_d T)\,[1+\gamma'(m)] & m \text{ is odd} \\ \exp(\mathrm{j}2\pi m f_d T)\,[1+\gamma'(m)] & m \text{ is even} \end{cases}, \tag{10}$$

$$\overline{f_d}_{X/Y} = \frac{1}{1/2L_{cazac}-2}\sum_{m=1}^{1/2L_{cazac}-2} 1/(4\pi T)\left[\arg\left(R'_{X/Y}(m+2)\right) - \arg\left(R'_{X/Y}(m)\right)\right]_{2\pi}. \tag{11}$$

It is worth noting that the legal range of the minus of $\arg\left(R'_{X/Y}\right)$ is 2π, which limits the maximum range of $\overline{f_d}$ to half of the baud rate. In order to detect positive/negative FO, we set this range to$(-\frac{1}{4}\text{baud}, \frac{1}{4}\text{baud})$.

CE: In contrast to typical random training sequences, the CAZAC sequence offers a distinct advantage with its unique flat spectrum, making it particularly advantageous for CE. In this section, we first estimate the frequency-dependent channel transfer function $H(\omega)$ in the whole signal bandwidth, which includes chromatic dispersion, polarization mode dispersion and band-limited effects. Then, we utilize $H(\omega)$ to calculate the initial equalizer coefficients via a zero-forcing method, which can accelerate or even skip the converging process of the equalizer. More details of the corresponding algorithms for CE can be found in [5].

3. Numerical and Experimental Results

Simulations and experiments are conducted with the same setup configurations. 15 GBaud dual-polarization 16 quadrature amplitude modulation (DP-16QAM) symbols with a length of 2^{15} serve as the payload of frame. At the beginning of the frame, the proposed preamble is added with a length of 272 (N=64, L=2 and N_{GI}=2). In the equalizer, the tap length and the block length are 128 and 64 (50% overlap), respectively, and 100 known blocks are used for convergence. Actually, the proposed preambles can provide accurate coefficients after CE, which necessitates fewer blocks for convergence.

The system is simulated with random time delays, FOs, SOPs, DGDs, clock jitters. Additive white Gaussian noise with a signal-to-noise ratio (SNR) of 19 dB and laser phase noise with a linewidth of 100 kHz are added. The FS and FOE results are shown in Fig.2(a-b). The timing metric of FS has a distinct peak to guarantee the correct synchronization, and the FOE error is below 0.4 MHz. As the SOP rotation angle θ and DGD increase, bit-error-ratio (BER) remains nearly constant with the aid of CE while BER without CE degrades severely as shown in Fig.2 (c-d).

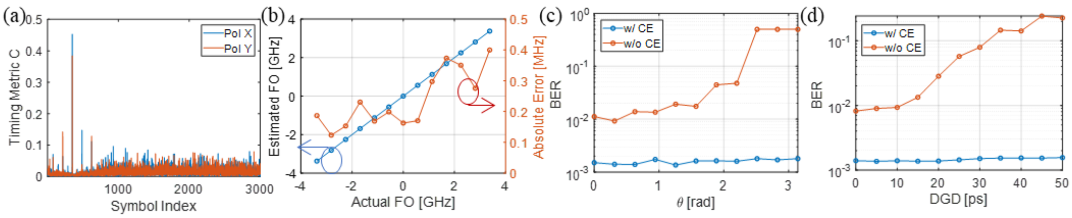

Fig.2 Numerical results. (a) Timing metric versus symbol index in FS. (b) Estimated FO and absolute FOE error versus actual FO. (c) BER versus SOP angle θ. (d) BER versus DGD with or without CE.

Fig. 3(a) depicts the experimental setup. The samples were loaded to an arbitrary waveform generator (AWG) after pulse shaping. An external cavity laser (ECL) was adopted with a 12.7 dBm optical power and a nominal linewidth of 50 kHz. Then, the electrical signals were fed into a DP in-phase and quadrature (IQ) transmitter. After being amplified to 0 dBm by an erbium-doped fiber amplifier (EDFA), the optical signal entered a 11 km standard single mode fiber. Then, the optical signal was attenuated by a variable optical attenuator (VOA) to adjust the received optical power (ROP) and then received by a coherent receiver. After sampled by a digital storage oscilloscope (DSO), the output signal was processed based on the burst-mode DSP offline. Fig. 3(b) shows the SNR versus ROP and Fig. 3(c) indicates that the maximum FOE error is below 1 MHz. As shown in Fig. 4(d-e), the equalizer with CE almost converges in the first few blocks whereas the equalizer without CE requires nearly 100 blocks to converge, inducing much more errors in the first 100 blocks. Fig. 3(f) shows the transfer functions after CE and LMS are almost overlapped, which explains the superior performance of the proposed scheme.

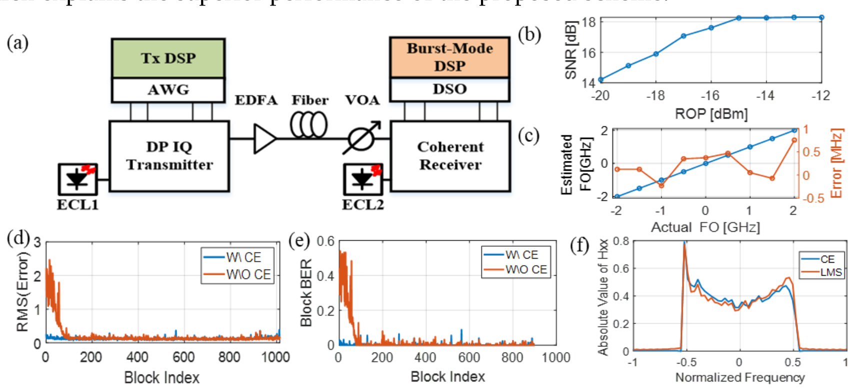

Fig.3 (a) Experimental setup. (b) Measured SNR versus ROP. (c) Estimated FO and absolute FOE error versus actual FO. (e) Root mean square (RMS) of errors versus block index. (f) BER of blocks versus block index. (g) Transfer function of the equalizer.

4. Conclusion

A preamble using a CAZAC sequence is proposed to jointly achieve FS, FOE and CE for the upstream burst-mode detection in coherent PON. In the simulation, the burst-mode DSP can work well in the presence of various FOs, SOPs and DGDs. In the experiment, precise FS and FOE can be achieved and the equalizer converges even in the first few blocks by utilizing a 272-symbol preamble.

Acknowledgment

This work was supported by National Key R&D Program of China (2022YFB2903500), Shanghai Pilot Program for Basic Research - Shanghai Jiao Tong University (21TQ1400213), and National Natural Science Foundation of China (62175145).

Reference

[1] J, Zhang, et al. IEEE Network, 36(2), 116-123 (2022).
[2] H. Wang, et al. J. Light. Technol., 41(14), 135-143 (2021).
[3] J. Zhang, et al. J. Opt. Commun. Netw., 13(2), A135-A143, (2021).
[4] U. Mengali, et al. IEEE Trans. Commun., 45(1), 23-25 (1997).
[5] F. Pittalà, et al. J. Light. Technol., 32(24), 4849-4863 (2014).